Inorganic Chemistry
Article

*Inorg. Chem.* **2009**, *48*, 6773–6780 **6773**
DOI: 10.1021/ic900718t

# Ab Initio Study of the Geometry, Stability, and Aromaticity of the Cyclic $S_2N_3^+$ Cation Isomers and Their Isoelectronic Analogues

**Guo-Hua Zhang,[†,§] Yong-Fang Zhao,[*,†] Judy I. Wu,[‡] and Paul v. R. Schleyer[*,‡]**

[†]*Center for Condensed Matter Science and Technology, Harbin Institute of Technology, Harbin 150001, People's Republic of China,* [‡]*Computational Chemistry Center, Department of Chemistry, University, of Georgia, Athens, Georgia 30602, and* [§]*Material Physics Department of Harbin University of Science and Technology, Harbin 150080, People's Republic of China*

Received April 13, 2009

A theoretical study of the geometries, energies, dissociation pathways, and aromaticity of the isomeric sulfur−nitrogen $S_2N_3^+$ rings reveals that the experimentally known 1,2-isomer is only stable kinetically. A rather high barrier inhibits its dissociation into the slightly lower energy $N_2$ and $NSS^+$ fragments via a stepwise mechanism. A second possible dissociation mode, into NNS and $NS^+$ via a concerted [3 + 2] mechanism, is endothermic. Instead, the reverse cycloaddition reaction has a low barrier and offers an exothermic route for the formation of cyclic 1,2-$S_2N_3^+$. Despite being thermodynamically more stable, the 1,3-isomer has only fleeting existence: its facile exothermic [3 + 2] cycloreversion into $N_2$ and $SNS^+$ fragments precludes observation. Nucleus independent chemical shifts (NICS) analysis reveals considerable six $\pi$ electron aromaticity for both cyclic $S_2N_3^+$ isomers, as well as their five membered ring valence isoelectronic analogues, $N_5^-$, $SN_4$, and $S_3N_2^{2+}$. The decomposition routes and the energetics of these analogues also provide comparisons along the series.

## 1. Introduction

Binary sulfur−nitrogen ring heterocycles have intrigued experimental[1−9] and theoretical[10−21] chemists since Gregory's[1] discovery of $S_4N_4$ in 1835. Chivers[10,11] and Oakley[12] have reviewed the preparation, behavior, geometries, and electronic structures of $S_xN_y$ ($x$, $y$ = 2−5) rings. $(SN)_x$ polymers with semimetallic and superconducting[22] properties are often used as starting materials for smaller sulfur−nitrogen compounds.[2−4] Hückel[23−25] molecular orbital theory and the concept of aromaticity is effective in predicting the composition of stable species and helping elucidate their properties.

This paper focuses on the smallest positively charged sulfur−nitrogen rings with six $\pi$ electrons, the five membered ring 1,3-$S_2N_3^+$ cation (**A**), and its 1,2-isomer (**B**) (Figure 1). The former is unknown experimentally but was considered in Bhattacharyya et al.'s[13] 1981 semiempirical CNDO/2 computational survey. Salts of the 1,2-isomer (**B**) were prepared and characterized by X-ray analysis independently by Herler et al.[8] and by Hass et al.[9] Herler's $\{[S_2N_3]^+\}_4[Hg_3Cl_{10}]^{4-}$ and $\{[S_2N_3]^+\}_2[Hg_2Cl_6]^{2-}$ salts were persistent at room temperature but decomposed at 80 °C; the geometry of the 1,2-isomer (**B**), computed at CCSD(T) and B3LYP levels, as well as a comparison of its aromatic $\pi$ molecular orbitals with those of the cyclopentadienyl anion $C_5H_5^-$, also were reported.

Since the more stable sulfur−nitrogen ring isomers generally have the maximum possible number of S−N bonds,[10,11] the energy of the 1,2-$S_2N_3^+$ isomer (**B**) should be higher than

*To whom correspondence should be addressed. E-mail: xgjing@hit.edu.cn (Y.-F. Z.), schleyer@chem.uga.edu (P.v.R.S.).

(1) Gregory, W. *J. Pharm.* **1835**, *21*, 315.
(2) Teichman, R. A.; Nixon, E. R. *Inorg. Chem.* **1976**, *15*, 1993.
(3) Hassanzadeh, P.; Andrews, L. *J. Am. Chem. Soc.* **1992**, *114*, 83.
(4) Lau, W. M.; Westwood, N. P. C.; Palmer, M. H. *J. Am. Chem. Soc.* **1986**, *108*, 3229.
(5) Roesky, H. W. *Angew. Chem., Int. Ed. Engl.* **1979**, *18*, 91.
(6) (a) Brooks, W. V. F.; Cameron, T. S.; Parsons, S.; Passmore, J.; Schriver, M. *J. Chem. Soc., Chem. Commun.* **1991**, *16*, 1079. (b) Brooks, W. V. F.; Cameron, T. S.; Parsons, S.; Passmore, J.; Schriver, M. J. *Inorg. Chem.* **1994**, *33*, 6230.
(7) Chivers, T.; Hojo, M. *Inorg. Chem.* **1984**, *23*, 1526.
(8) Herler, S.; Mayer, P.; Nöth, H.; Schulz, A.; Suter, M.; Vogt, M. *Angew. Chem., Int. Ed.* **2001**, *40*, 3173.
(9) Haas, A. *Z. Anorg. Allg. Chem.* **2002**, *628*, 673.
(10) Chivers, T. *Acc. Chem. Res.* **1984**, *17*, 166.
(11) Chivers, T. *Chem. Rev.* **1985**, *85*, 341.
(12) Oakley, R. T. *Prog. Inorg. Chem.* **1988**, *36*, 299.
(13) Bhattacharyya, A. A.; Bhattacharyya, A.; Adkins, R. R.; Turner, A. G. *J. Am. Chem. Soc.* **1981**, *103*, 7458, and references therein.
(14) Tuononen, H. M.; Suontamo, R.; Valkonen, J.; Laitinen, R. *J. Phys. Chem. A* **2004**, *108*, 5670.
(15) Klapötke, T. M.; Jiabo, L.; Harcourt, R. D. *J. Phys. Chem. A* **2004**, *108*, 6527.
(16) Adkins, R. R.; Turner, A. G. *J. Am. Chem. Soc.* **1978**, *100*, 1383.
(17) Gimarc, B. M.; Warren, D. S. *Inorg. Chem.* **1991**, *30*, 3276.
(18) Parsons, S.; Passmore, J. *Acc. Chem. Res.* **1994**, *27*, 101.
(19) Chandler, G. S.; Jayatilaka, D.; Wajrak, M. *J. Chem. Phys.* **1995**, *198*, 169.
(20) Boere, R. T.; Tuononen, H. M.; Chivers, T.; Roemmele, T. L. *J. Organomet. Chem.* **2007**, *692*, 2683.
(21) Grein, F. *Can. J. Chem.* **1992**, *71*, 335.
(22) Greene, R. L.; Street, G. B. *Phys. Rev. Lett.* **1975**, *34*, 577.
(23) Hückel, E. *Z. Phys.* **1932**, *76*, 628.
(24) Breslow, R.; Mohacsi, E. *J. Am. Chem. Soc.* **1963**, *85*, 431.
(25) Klein, D. J.; Trinajstic, N. *J. Am. Chem. Soc.* **1984**, *106*, 8050.


Published on Web 06/04/2009

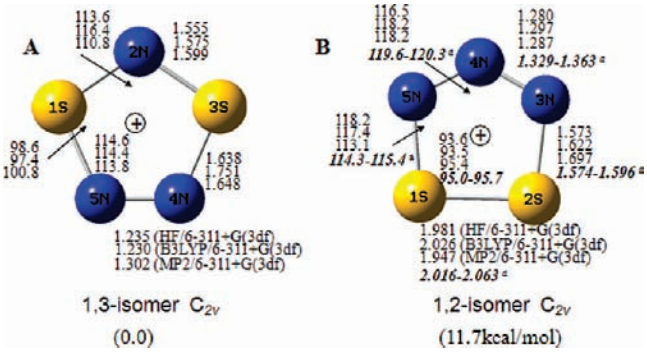


**Figure 1.** Geometries and relative energies (computed at the MP2/6-311+G(3df) level) of 1, 3- (**A**) and 1, 2- (**B**) $S_2N_3^+$ isomers. The experimental data ([a]) correspond to complex salts rather than to the free ion (ref. 8).

that of the 1,3-isomer (**A**). Why then is the 1,3-$S_2N_3^+$ isomer (**A**) unknown? Is this because of some unexpected instability or merely to an oversight of preparative chemistry? We address these questions here. The five membered $N_5^-$, $SN_4$, and $S_3N_2^{2+}$ rings also are considered to compare the entire related six $\pi$ electron series.

Like their carbocyclic counterparts, planar sulfur−nitrogen ring systems with $4N+2$ $\pi$-electrons (each sulfur atom contributes two, each nitrogen one) are stabilized by aromaticity and exhibit characteristic magnetic properties due to induced diatropic ring currents. The four-membered $N_2S_2$ ring, studied by Jung et al.,[26] is the smallest 6 $\pi$ e example, but ring current probes have demonstrated the aromaticity of numerous sulfur−nitrogen compounds, including $S_2N_2$, $S_3N_3^-$, $S_4N_3^+$, $S_4N_4^{2+}$, and $S_5N_5^+$.[27] Nucleus independent chemical shifts (NICS) aromaticity probes, introduced in 1996[28] and developed considerably since,[29−37] are particularly effective.[26,27] Canonical molecular orbital NICS (CMO-NICS) analysis has been employed here to delineate the aromaticity of the 1,2- and 1,3-$S_2N_3^+$, as well as that of their six $\pi$ electron five membered ring analogues.

## 2. Computational Methods

All geometries were optimized at both the B3LYP/6-311+G(3df)[38,39] and MP2/6-311+G(3df)[40] level as implemented in the Gaussian 03 program.[41] Harmonic vibrational frequency computations verified minima (all-real frequencies) and transition structures (one imaginary frequency), and provided the zero point energy (ZPE) corrections (scaled by 0.9806 as recommended by Scott and Radom).[42] Intrinsic reaction coordinates (IRC)[43,44] potential energy surface computations using the Gonzalez−Schlegel second-order algorithm confirmed the dissociation products. NICS[28−37] computations at GIAO[45]-MP2/6-311+G(3df)//PW91/IGLOIII established the aromaticity of the cyclic $S_2N_3^+$ isomers by comparison to the cyclopentadienyl anion $C_5H_5^-$ and benzene. Both the isotropic NICS[28] and the dissected canonical molecular orbital (CMO)-NICS[34−36] were computed with NICS points located at the ring center, NICS(0),[28] and at 1 Å above the ring center, NICS(1).[27] CMO-NICS, evaluated using the gauge individual atomic orbital (GIAO) method,[45] dissects the isotropic NICS into the contributions of each of the canonical molecular orbitals.[35−37] We employ the most sohisticated NICS aromaticity index, $NICS_{\pi zz}$,[32−34] which is based on the out-of-plane ($zz$) tensor component of the isotropic NICS and includes only contributions from the $\pi$ CMOs. Negative NICS values in and above aromatic ring systems indicate aromaticity; positive NICS values are associated with antiaromaticity.

## 3. Results and Discussion

**3.1. Geometries.** Both of the five-membered ring $S_2N_3^+$ isomers (**A**) and (**B**) (in Figure 1) have singlet ground states. The triplet 1,2-$S_2N_3^+$ (**B**) is about 67.0 kcal/mol higher in energy than the singlet at MP2/6-311+G(3df). The optimized geometrical parameters of isomers (**A**) and (**B**) at HF, B3LYP, and MP2 levels (with the 6-311+G(3df) basis set) are shown in Figure 1, along with the experimental data of the 1,2-isomer **B** discussed by Herler.[8] Note that the 1,3-isomer (**A**) has two kinds of S−N bonds. The one between the single nitrogen and a sulfur (S1−N2) ranges from 1.56 Å to 1.60 Å, and is closer to the double (1.54 Å) than the single (1.74 Å) SN bond length. The SN bond to the $N_2$ unit (S1−N5) is longer and corresponds more closely to a single SN bond. The NN distances in both **A** and **B** are in the 1.23 to 1.30 Å range between a single and a double NN bond.

**3.2. Dissociation Pathways, Kinetic, and Thermodynamic Stabilities.** Although 1,2-$S_2N_3^+$ (**B**) has been observed experimentally,[8] 1,3-$S_2N_3^+$ (**A**) is 11.7 kcal/mol more stable energetically (Table 1). 1,3-$S_2N_3^+$ (**A**) may be favored by having a greater degree of S and N alternation in the ring, as well as having less lone pair repulsion

(26) Jung, Y.; Heine, T.; Schleyer, P. v. R.; Head-Gordon, M. *J. Am. Chem. Soc.* **2004**, *126*, 3132.
(27) (a) De Proft, F.; Fowler, P. W.; Havenith, R. W. A.; Schleyer, P. v. R.; Lier, G. V.; Geerlings, P. *Chem.—Eur. J.* **2004**, *10*, 940. (b) Cossio, F. P.; Morao, I.; Jiao, H. J.; Schleyer, P. v. R. *J. Am. Chem. Soc.* **1999**, *121*, 6737.
(28) Schleyer, P. v. R.; Maerker, C.; Dransfeld, A.; Jiao, H.; Hommes, N. J. P. v. E. *J. Am. Chem. Soc.* **1996**, *118*, 6317.
(29) Schleyer, P. v. R.; Jiao, H.; Hommes, N. J. R. v. E.; Malkin, V. G.; Malkina, O. L. *J. Am. Chem. Soc.* **1997**, *119*, 12669.
(30) Cyranski, M. K.; Krygowski, T. M.; Katritzky, A. R.; Schleyer, P. v. R. *J. Org. Chem.* **2002**, *67*, 1333.
(31) Corminboeuf, C.; Heine, T.; Weber, J. *Phys. Chem. Chem. Phys.* **2003**, *5*, 246.
(32) Corminboeuf, C.; Heine, T.; Seifert, G.; Schleyer, P. v. R. *Phys. Chem. Chem. Phys.* **2004**, *6*, 273.
(33) Chen, Z. F.; Wannere, C. S.; Corminboeuf, C.; Puchta, R.; Schleyer, P. v. R. *Chem. Rev.* **2005**, *105*, 3842.
(34) Fallah-Bagher-Shaidaei, H.; Wannere, C. S.; Corminboeuf, C.; Puchta, R.; Schleyer, P. v. R. *Org. Lett.* **2006**, *8*, 863.
(35) Corminboeuf, C.; Heine, T.; Weber *J. Org. Lett.* **2003**, *5*, 1127.
(36) Moran, D.; Manoharan, M.; Heine, T.; Schleyer, P. v. R. *Org. Lett.* **2003**, *5*, 23.
(37) Heine, T.; Schleyer, P. v. R.; Corminboeuf, C.; Seifert, G.; Reviakine, R.; Weber, J. *J. Phys. Chem.* **2003**, *107*, 6470.
(38) Becke, A. D. *J. Chem. Phys.* **1993**, *98*, 1372.
(39) Lee, C.; Yang, W.; Parr, R. G. *Phys. Rev. B* **1988**, *37*, 785.
(40) Møller, C.; Plesset, M. S. *Phys. Rev.* **1934**, *46*, 618.
(41) Frisch, M. J.; Trucks, G. W.; Schlegel, H. B.; Scuseria, G. E.; Robb, M. A.; Cheeseman, J. R.; Montgomery, J. A. Jr.; Vreven, T.; Kudin, K. N.; Burant, J. C.; Millam, J. M.; Iyengar, S. S.; Tomasi, J.; Barone, V.; Mennucci, B.; Cossi, M.; Scalmani, G.; Rega, N.; Petersson, G. A.; Nakatsuji, H.; Hada, M.; Ehara, M.; Toyota, K.; Fukuda, R.; Hasegawa, J.; Ishida, M.; Nakajima, T.; Honda, Y.; Kitao, O.; Nakai, H.; Klene, M.; Li, X.; Knox, J. E.; Hratchian, H. P.; Cross, J. B.; Bakken, V.; Adamo, C.; Jaramillo, J.; Gomperts, R.; Stratmann, R. E.; Yazyev, O.; Austin, A. J.; Cammi, R.; Pomelli, C.; Ochterski, J. W.; Ayala, P. Y.; Morokuma, K.; Voth, G. A.; Salvador, P.; Dannenberg, J. J.; Zakrzewski, V. G.; Dapprich, S.; Daniels, A. D.; Strain, M. C.; Farkas, O.; Malick, D. K.; Rabuck, A. D.; Raghavachari, K.; Foresman, J. B.; Ortiz, J. V.; Cui, Q.; Baboul, A. G.; Clifford, S.; Cioslowski, J.; Stefanov, B. B.; Liu, G.; Liashenko, A.; Piskorz, P.; Komaromi, I.; Martin, R. L.; Fox, D. J.; Keith, T.; Al-Laham, M. A.;. Peng, C. Y; Nanayakkara, A.; Challacombe, M.; Gill, P. M. W.; Johnson, B.; Chen, W.; Wong, M. W.; Gonzalez, C.; Pople, J. A. *Gaussian03*, Revision C.02; Gaussian, Inc.: Wallingford, CT, 2004.
(42) Scott, A. P.; Radom, L. *J. Phys. Chem.* **1996**, *100*, 16502.
(43) Gonzalez, C.; Schlegel, H. B. *J. Chem. Phys.* **1989**, *90*, 2154.
(44) Gonzalez, C.; Schlegel, H. B. *J. Phys. Chem.* **1990**, *94*, 5523.
(45) Ditchfield, R. *Mol. Phys.* **1974**, *27*, 789.

**Table 1.** Total Energies (in hartrees) and Unscaled Zero-Point Energies (in Parentheses) of the Structures (SS), Transition States (TS), and Dissociation Products (P) of 1,3-$S_2N_3^+$ (**A**) and 1,2-$S_2N_3^+$ (**B**)[a]

| | total energies (ZPE in kcal/mol) | relative energies (with scaled ZPE) |
|---|---|---|
| **1,3-$S_2N_3^+$ (A)** | | |
| **A**-SS | −959.03442 (9.4) | 0.0[−11.7][b] |
| **A**-TS1 | −959.02888 (8.7) | 2.6 |
| **A**-TS2 | −959.01050 (8.6) | 15.8 |
| **A**-P1 ($SNS^+ + N_2$) | −959.11907 (7.7) | −51.3 |
| **A**-P2 ($SNN + NS^+$) | −959.11410 (7.0) | −52.4 |
| **A**-P3 ($NSN + NS^+$) | −958.88553 (6.4) | 93.4 |
| **1,2-$S_2N_3^+$ (B)** | | |
| **B**-SS1 | −959.01529 (9.1) | 0.0 |
| **B**-TS1 | −958.98977 (8.7) | 15.6 |
| **B**-TS21 | −959.00344 (9.4) | 7.7 |
| **B**-SS2 | −959.01268 (9.4) | 1.9 |
| **B**-TS22 | −958.95671 (7.1) | 34.9 |
| **B**-P1 ($NNS + NS^+$) | −958.99959 (7.1) | 10.0 |
| **B**-P2 ($N_2 + SNS^+$) | −959.01346 (6.4) | −1.6 |
| **B**-P3 ($S_2^{2+} + N_3^-$) | −958.42590 (7.5) | 368.3 |
| **B**-P4 ($S_2 + N_3^+ D_{3h}$) | −958.78603 (6.2) | 141.1 |

[a] The relative energies (including ZPE corrections scaled by 0.9806) of the transition states and dissociation products also are listed. All geometries were optimized at the MP2/6-311 + G(3df) level. [b] Energy relative to 1,2-$S_2N_3^+$ (**B**-SS1)

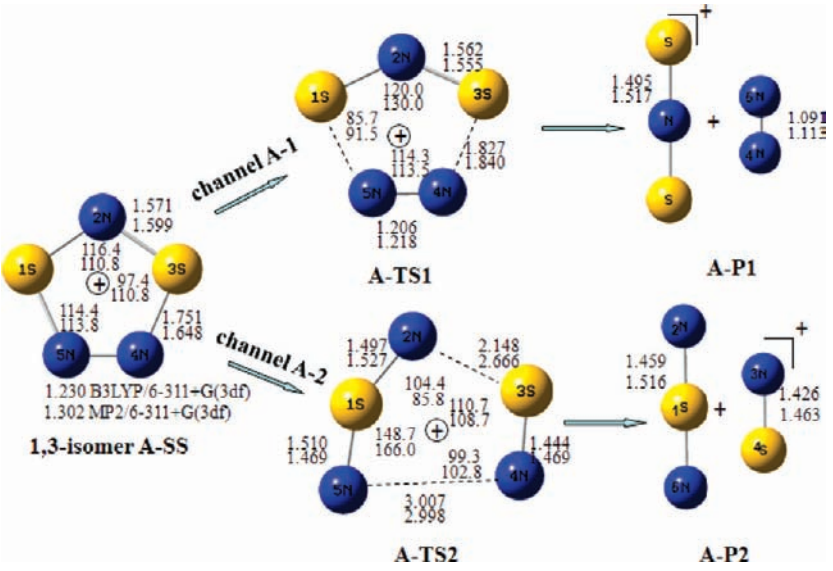


**Figure 2.** Optimized geometries (bond lengths in Å; bond angles in degrees) of species involved in the 1,3-$S_2N_3^+$ (**A**) dissociation channels.

between vicinal N atoms (there is one NN unit in **A** but two in **B**). However, being thermodynamically more favorable does not necessarily result in greater kinetic persistence.[46] Just the opposite is true here. The "kinetic stability" of **A** (Figure 2) and **B** (Figure 3) were compared by computing the barriers of their various dissociation channels (see also Table 1 for energetic data).

**3.2.1. 1,3-Isomer $S_2N_3^+$ (A).** The symmetrical [3 + 2] $C_{2v}$ cycloreversion (channel **A**1 in Figure 2) of 1,3-$S_2N_3^+$ (**A**), via simultaneous S−N bond elongation, leads to $SNS^+$ and $N_2$ (**A**-P1) and is exothermic by 51.3 kcal/mol. Notably, the **A**1 dissociation barrier (2.6 kcal/mol), via **A**-TS1, is even less than the ZPE correction (8.7 kcal/mol)! Thus, 1,3-$S_2N_3^+$ (**A**) could dissociate quite readily in experiment, which precludes its detection. The asymmetrical dissociation channel (**A**2), involving synchronous S3−N4 and S1−N2 bond breaking, gives NNS and NS+, but has a substantially higher barrier 15.6 kcal/mol (via **A**-TS2). A third possible dissociation pathway, involving N−N bond breaking leading to NSN and $NS^+$, is endothermic by 93.4 kcal/mol and thus is not considered further here.

**3.2.2. 1, 2-Isomer $S_2N_3^+$ (B).** As shown in Figure 3, **B**1 represents the [3 + 2] cycloreversion of 1,2-$S_2N_3^+$ (**B**-SS1) via transition state (**B**-TS1) into the NNS and NS+ products (**B**-P1). This result is confirmed by IRC computations. The **B**1 pathway is endothermic by 10.1 kcal/mol but has a 15.6 kcal/mol dissociation barrier. Thus, the reverse (cycloaddition) barrier is only 5.5 kcal/mol. Consequently, NNS and $NS^+$ are likely precursors for the formation of 1,2-$S_2N_3^+$ in Herler's experiments.[8]

The **B**2 dissociation pathway is slightly exothermic (−1.6 kcal/mol) and gives $N_2$ and $NSS^+$ (**B**-P2) in two consecutive steps. The first step involves ring-opening through S1N5 bond rupture and leads to **B**-SS2 (only 1.9 kcal/mol higher in energy than **B**-SS1). The barrier for this step (via **B**-TS21) is 7.7 kcal/mol, and, with the exception of the S1N5 separation, little change in bond

(46) Hoffmann, R.; Schleyer, P. v. R.; Schaefer, H. F.III *Angew. Chem., Int. Ed.* **2008**, *47*, 2.

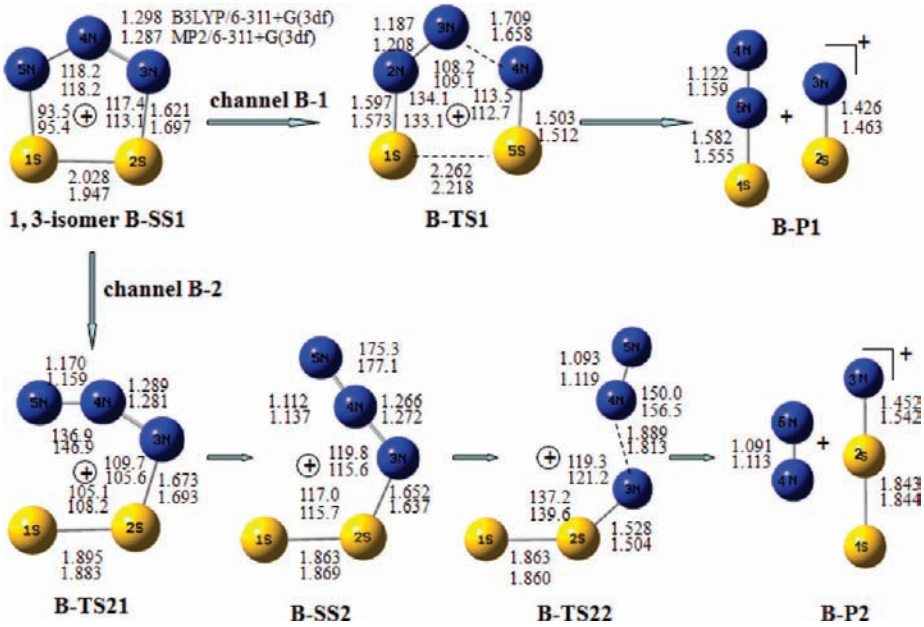


**Figure 3.** Optimized geometries (bond lengths in Å; bond angles in degrees) of the species involved in the 1,2-$S_2N_3^+$ **(B)** dissociation channels.

lengths takes place. The second step involves the N3−N4 bond cleavage of **B**-SS2 (via **B**-TS22) to give **B**-P2. On the basis of IRC computations, the N4−N5 and S2−N3 bonds shorten significantly as the N3N4 distance increases. At the **B**-TS22 transition state, the N4−N5 bond length (1.119 Å) is comparable to the experimental triple bond length of $N_2$ (1.098 Å). The dissociation barrier (34.9 kcal/mol) for this step is significant and contributes to the experimental persistence of 1,2-$S_2N_3^+$.[8]

The [3 + 2] cycloreversions of 1, 2-$S_2N_3^+$ (**B**) leading to $S_2^{2+} + N_3^-$ (**B**-P3) or to $N_3^+$ (a $D_{3h}$ symmetry singlet) + $S_2$ (**B**-P4) are extremely endothermic and thus are unrealistic. The formation of **B**-P3 involves the simultaneous elongation of two N−S bonds but is 368.3 kcal/mol higher in energy than 1,2-$S_2N_3^+$ (**B**). The formation of $N_3^+$ (a $D_{3h}$ symmetry singlet) + $S_2$ (**B**-P4) is more favorable Coulombically, but these products are still 141.1 kcal/mol higher in energy than 1,2-$S_2N_3^+$ (**B**).

Despite being thermochemically more stable than (**B**), 1,3-$S_2N_3^+$ (**A**) dissociates (into linear S=N=S$^+$ and $N_2$) readily; its low barrier precludes observation. In contrast, all the possible dissociation channels of the 1,2-isomer (**B**) have high barriers. Thus, attempts to detect $S_2N_3^+$ give the metastable (higher energy, but kinetically viable) 1,2-isomer (**B**) rather than the thermodynamically more stable (lower energy) 1,3-isomer (**A**). (This is a cogent example of the need to define what "stable" means when used in a scientific context.)[46]

**3.3. Related Species: $N_5^-$, $SN_4$, and $S_3N_2^{2+}$.** For comparison, we also evaluated the possible dissociation pathways of related five membered rings with six $\pi$ electrons, $N_5^-$ (**C**), $SN_4$ (**D**), 1,3- $S_3N_2^{2+}$ (**E**), and 1,2-$S_3N_2^{2+}$ (**F**). The geometries of the species involved in the dissociation channels are presented in Figures 4−7, respectively. Figure 8 depicts the dissociation channels schematically of the related species together with 1,2- (**B**) and 1,3-$S_2N_3^+$ (**A**) isomer.

**3.3.1. $N_5^-$.** The pentazolate anion $N_5^-$ has been detected experimentally[47] and has been studied extensively[47−51] because of its potential use as a high-energy high-density material (HEDM). The dissociation of $N_5^-$ into $N_2$ and $N_3^-$ (**C**-P) is only modestly exothermic (12.7 kcal/mol) but has a 24.9 kcal/mol barrier via transition state **C**-TS (see Table 2). Like its $C_5H_5^-$ hydrocarbon counterpart, $N_5^-$ is highly aromatic (see Nucleus Independent Chemical Shifts section). The NN distance in $D_{5h}$ $N_5^-$ (1.334 Å at the MP2/6-311+G(3df) level), between the usual NN single and double bond lengths, documents the extensive six $\pi$ electron delocalization.

**3.3.2. $SN_4$.** $SN_4$ has three conceivable sets of fragmentation products, **D**-P1 (NNS + NN), **D**-P2 (NSN + NN), and **D**-P3 ($NNN^- + NS^+$) (see Table 2 and Figure 5). The most facile dissociation pathway, **D**1, leading to NNS + NN (**D**-P1, Figure 5), is exothermic by 137.2 kcal/mol and has a 7.0 kcal/mol barrier via a $C_{2v}$ **D**-TS1 transition state (see Figure 5).[52] Alternative dissociation pathways (**D**2 and **D**3) are unfavorable. The **D**-P2 products (NSN + NN) are 5.3 kcal/mol less stable than $SN_4$ and the **D**2 dissociation barrier is 34.4 kcal/mol. The **D**-P3 ($NNN^- + NS^+$) dissociation is endothermic by 193.7 kcal/mol.

**3.3.3. $S_3N_2^{2+}$.** In 1991, Passmore et al. characterized the 1,3-$S_3N_2^{2+}$ isomer (**E**-SS in Figure 6),[6a,20] which follows the alternating S, N atom rule.[10−12] Indeed, 1,2-$S_3N_2^{2+}$ (**F** in Figure 7, evidently studied here for the first time) is

(47) Vij, A.; Pavlovich, J. G.; Wilson, W. W.; Vij, V.; Christe, K. O. *Angew. Chem., Int. Ed.* **2002**, *41*, 3051.
(48) Glukhovtsev, M. N.; Jiao, H.; Schleyer, P. v. R. *Inorg. Chem.* **1996**, *35*, 7124.
(49) Tsipis, A. C.; Chaviara, A. T. *Inorg. Chem.* **2004**, *43*, 1273.
(50) Christe, K. O. *Propellants, Explosives, Pyrotechnics* **2007**, *32*, 194.
(51) Dixon, D. A.; Feller, D.; Christe, K. O.; Wilson, W. W.; Vij, A.; Vij, V.; Jenkins, H. D. B.; Olson, R. M.; Gordon, M. S. *J. Am. Chem. Soc.* **2004**, *126*, 834.
(52) Wang, L. J.; Mezey, P. G.; Zgierski, M. Z. *Chem. Phys. Lett.* **2003**, *369*, 386.

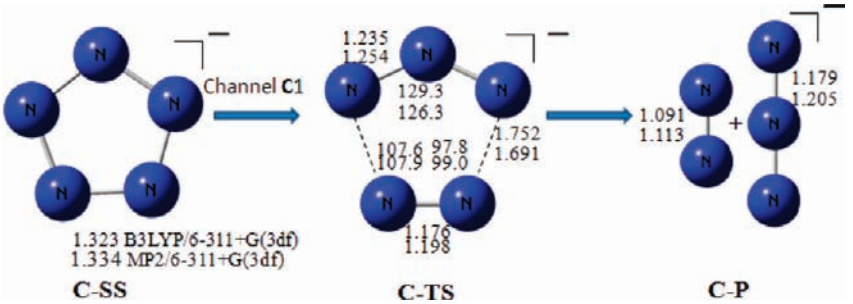


**Figure 4.** Optimized geometries (bond lengths in Å; bond angles in degrees) of the species involved in the dissociation of $N_5^-$ **(C)**.

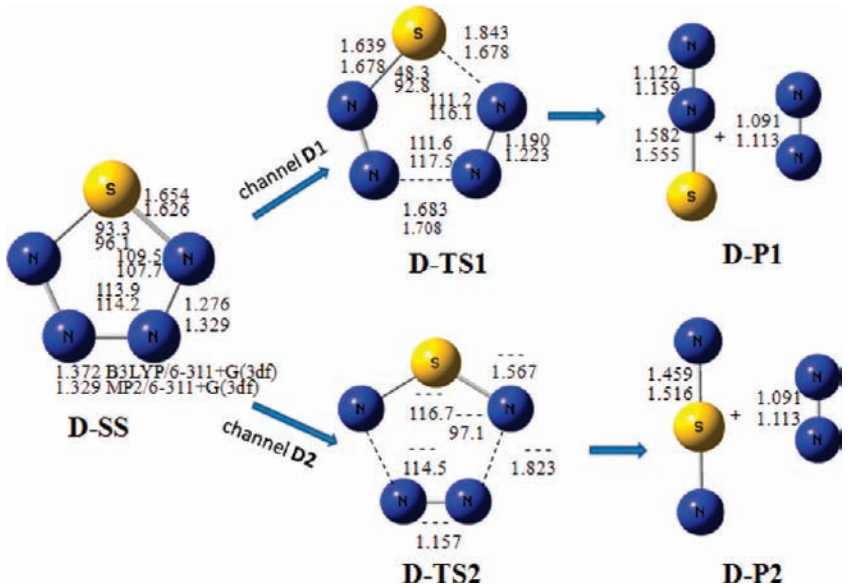


**Figure 5.** Optimized geometries (bond lengths in Å; bond angles in degrees) of the species involved in the $SN_4$ **(D)** dissociation channels.

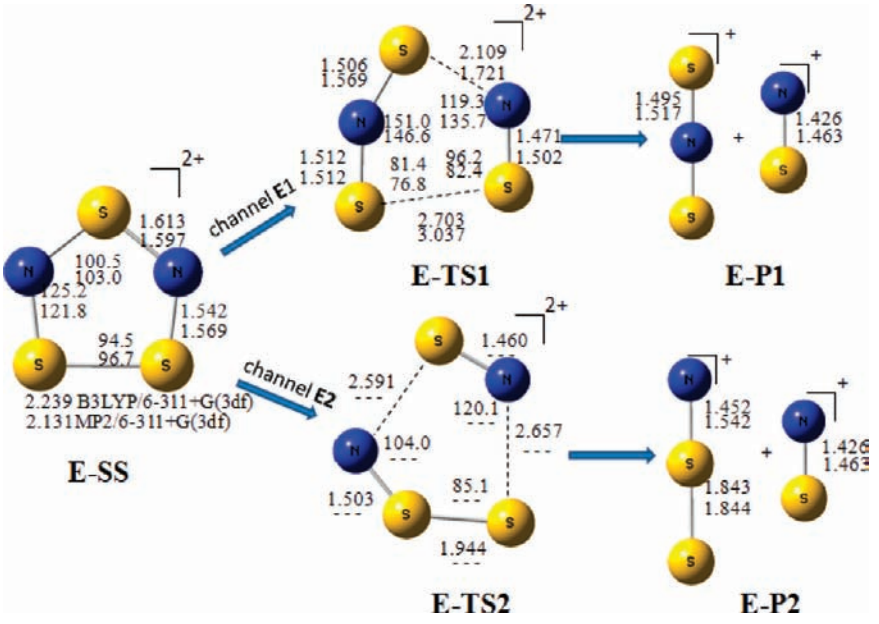


**Figure 6.** Optimized geometries (bond lengths in Å; bond angles in degrees) of the species involved in the dissociation channels of 1,3- $S_3N_2^{2+}$ **(E)**.

16.2 kcal/mol higher in energy (see Table 2). 1,3-$S_3N_2^{2+}$ dissociates readily into $NS^+$ and $SNS^+$ fragments in liquid $SO_2$ because of the large exothermicity (in the absence of crystal lattice energy) and the rather low barrier (less than 20 kcal/mol as computed by Grein in his detailed 1993 theoretical study).[21] We find this dissociation pathway

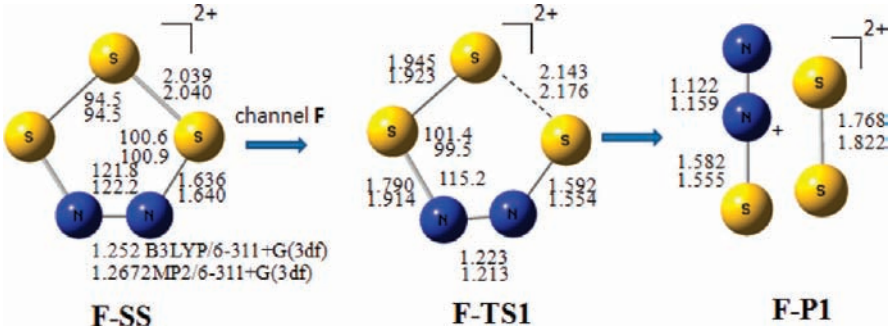


**Figure 7.** Optimized geometries (bond lengths in Å; bond angles in degrees) of the species involved in the dissociation of 1,2-$S_3N_2^{2+}$ (**F**).

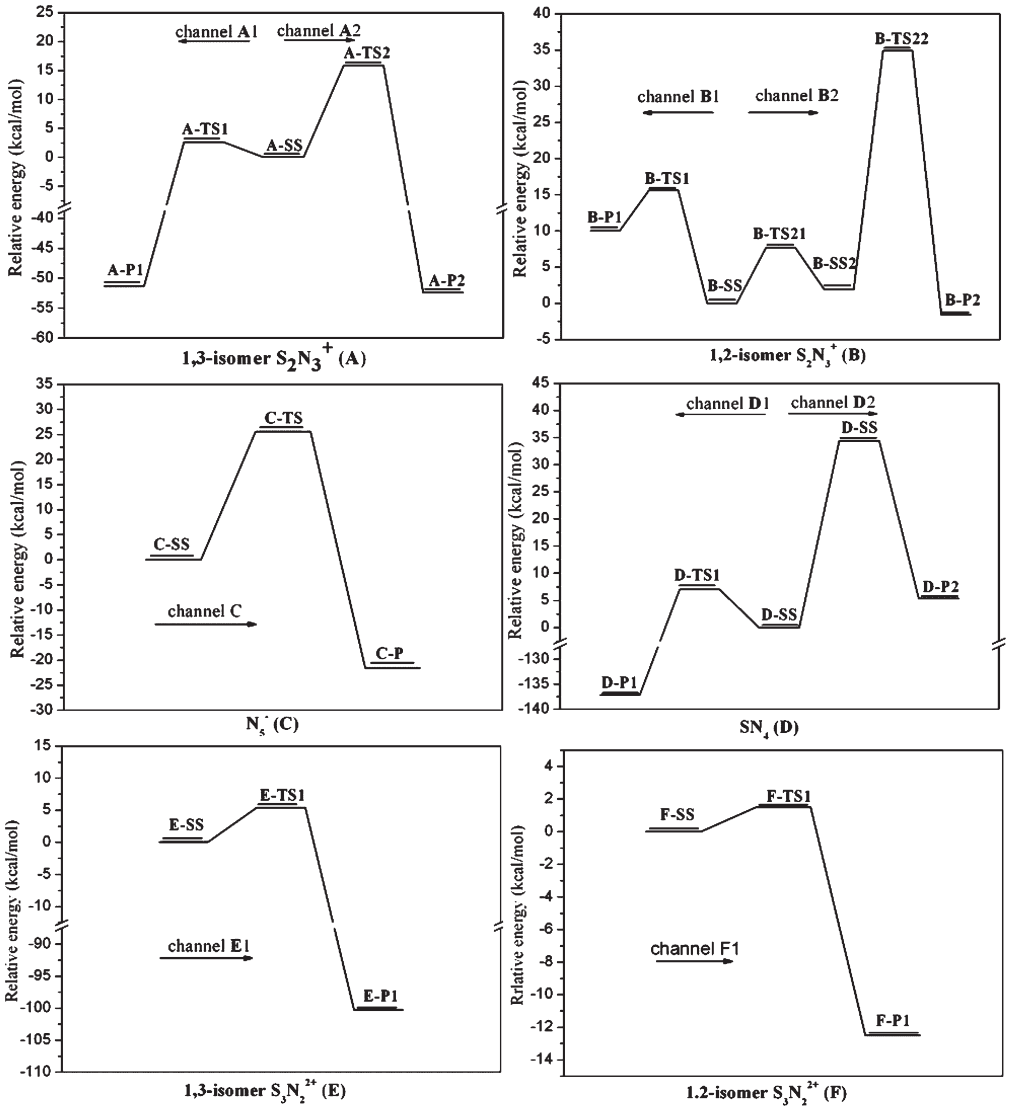


**Figure 8.** Schematic representations of the various dissociation channels of 1,3-$S_2N_3^+$ (**A**), 1,2-$S_2N_3^+$ (**B**), $N_5^-$ (**C**), $SN_4$ (**D**), 1,3-$S_3N_2^{2+}$ (**E**), and 1,2-$S_3N_2^{2+}$ (**F**). Note the differences in the energy scaling.

(**E**1, see Figure 6) to be exothermic by 100.3 kcal/mol with an energy barrier of only 5.4 kcal/mol. All other possible 1,3-$S_3N_2^{2+}$ dissociation routes have higher energy barriers. The **E**2 pathway, resulting in $NSS^+ + NS^+$ (**E**-P2), is exothermic by 35.1 kcal/mol but is precluded by an 81.2 kcal/mol dissociation barrier (via **E**-TS2); E3 leads to $NSN + SS^{2+}$ (**E**-P3) and is endothermic by 146.2 kcal/mol. In contrast, the dissociation barrier of 1,2-$S_3N_2^{2+}$ (**F**-SS) into $SS^{2+} + SNN$ (**F**-P1) is very low (1.5 kcal/mol) (see Figure 7). Thus, the known 1,3-$S_3N_2^{2+}$ isomer not only is thermodynamically more stable but also is more persistent kinetically than its 1,2-isomer.

**3.4. Molecular Orbital Analysis.** Some of the 1,2-$S_2N_3^+$ (**B**) MOs were related schematically to those of the isoelectronic $C_5H_5^-$ by Herler et al.[8] Our canonical $\pi$ MO (CMO-NICS) comparison (see Figure 9) shows

**Table 2.** Total Energies (in hartrees) and Unscaled Zero-Point Energies (in parentheses) of the Structures (SS), Transition States (TS), and Dissociation Products (P) of $N_5^-$ (**C**), $SN_4$ (**D**), 1,3-$S_3N_2^{2+}$ (**E**), and 1,2-$S_3N_2^{2+}$ (**F**)[a]

| | total energies (ZPE in kcal/mol) | relative energies (with scaled ZPE) |
|---|---|---|
| **$N_5^-$ (C)** | | |
| **C**-SS | −273.30741 (13.3) | 0.0 |
| **C**-TS | −273.26319 (11.1) | 25.6 |
| **C**-P($NNN^- + N_2$) | −273.33597 (9.6) | −21.6 |
| **$SN_4$ (D)** | | |
| **D**-SS | −616.27454 (11.2) | 0.0 |
| **D**-TS1 | −616.26036 (9.2) | 7.0 |
| **D**-TS2 | −616.21878 (10.6) | 34.4 |
| **D**-P1(NNS + NN) | −616.48869 (8.3) | −137.2 |
| **D**-P2(NSN + NN) | −616.26007 (7.3) | 5.3 |
| **D**-P3($NNN^- + NS^+$) | −615.96143 (8.5) | 193.7 |
| **1,3-$S_3N_2^{2+}$ (E)** | | |
| **E**-SS | −1301.58811 (8.5) | 0.0[−16.2][b] |
| **E**-TS1 | −1301.57795 (7.5) | 5.4 |
| **E**-TS2 | | 81.2[c] |
| **E**-P1($SNS^+ + NS^+$) | −1301.74453 (6.3) | −100.3 |
| **E**-P2($NSS^+ + NS^+$) | −1301.63892 (5.1) | −35.1 |
| **E**-P3($NSN + SS^{2+}$) | −1301.34999 (5.2) | 146.2 |
| **1,2-$S_3N_2^{2+}$ (F)** | | |
| **F**-SS | −1301.56101 (7.6) | 0.0 |
| **F**-TS1 | −1301.55812(7.3) | 1.5 |
| **F**-P1($NNS + SS^{2+}$) | −1301.57862 (7.2) | −12.5 |
| **F**-P2($NN + SSS^{2+}$) | −1301.56027 (5.7) | −1.5 |
| **F**-P3($SSN^+ + NS^+$) | −1301.63892 (5.1) | −53.3 |

[a] The relative energies (including ZPE corrections scaled by 0.9806) of the transition states and dissociation products also are listed. All geometries were optimized at the MP2/6-311 + G(3df) level. [b] Energy relative to 1,2-$S_3N_2^{2+}$ (**F-SS**). [c] Computed at the B3LYP/6-311 + G(3df) level.

that 1,3-$S_2N_3^+$ (**A**) is quite similar to both of these (see discussion below). All 13 occupied valence (and some virtual) MOs of 1,2-$S_2N_3^+$ are shown in Figure 9 (the MOs of the 1,3-isomer (**B**) are analogous). The $\sigma$-bonding framework is composed of s-AO S and N combinations (MOs $7a_1$, $6b_1$, $8a_1$, $7b_1$, and $9a_1$) as well as of in-plane $\pi$-AO S and N combinations) MOs $10a_1$, $8b_1$, $11a_1$, $9b_1$, $12a_1$. MOs $2b_2$, $3b_2$, and $2a_2$ are the three occupied $\pi$ orbitals formed from the out-of-plane $\pi$ AOs of sulfur and nitrogen (also shown in Figure 10). MOs $3a_2$ and $4a_2$ are two of the unoccupied $\pi$ orbitals.

**3.5. Nucleus Independent Chemical Shifts (NICS).** NICS computations reveal that both (**A**) and (**B**) are almost as aromatic as the isoelectronic cyclopentadienyl anion, $C_5H_5^-$, based on the most sophisticated $NICS_{\pi zz}$ index. Both (**A**) (−30.6 ppm) and (**B**) (−30.5 ppm) have large negative $NICS(0)_{\pi zz}$ values (in the ring centers) only slightly smaller than $D_{5h}$ $C_5H_5^-$ (−35.3) and $D_{6h}$ benzene (−36.2 ppm) (see Table 3). The weaker magnetic aromaticity of (**A**) and (**B**) is expected geometrically, in view of their bond length alternation (see Table 1), nonuniformity of the ring atoms, and larger average ring radii.

Note that some of the other NICS indexes, in contrast to $NICS(0)_{\pi zz}$, may give misleading conclusions.[33,34] For example, the isotropic NICS(0) for (**A**) (−18.9 ppm) and for (**B**) (−23.3 ppm) suggest erroneously that both are distinctly more aromatic than $C_5H_5^-$ (NICS(0) = −12.9 ppm) and benzene (NICS(0) = −7.5 ppm) (Table 3). Isotropic NICS(0) values are strongly influenced by the local sigma contributions of the ring, which (unlike the $\pi$ effects) are not related to aromaticity.[33,34] $NICS(0)_{zz}$ extracts the out-of-plane tensor component of the isotropic NICS but is also largely offset by the $\sigma$ orbital contributions ($NICS(0)_{\sigma zz}$). Thus, the $NICS(0)_{zz}$ values for (**A**) (−45.4 ppm) and (**B**) (−54.0 ppm) are more negative than those of $C_5H_5^-$ (−17.3 ppm) and benzene (−15.0 ppm). Note that the $NICS(0)_{\sigma zz}$ values are negative (diatropic) for (**A**) (−14.8 ppm) and (**B**) (−23.5 ppm) but positive (paratropic) for $C_5H_5^-$ (+18.0 ppm) and benzene (+21.2 ppm).

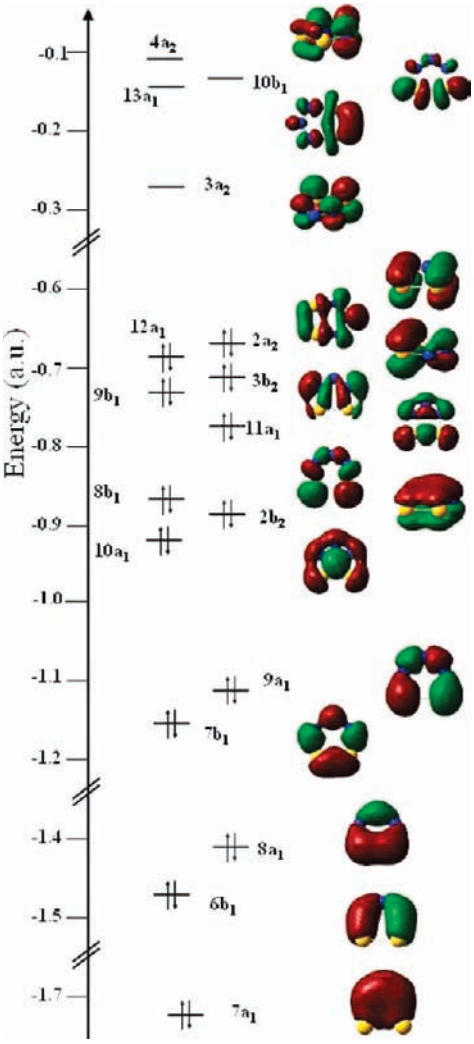


**Figure 9.** Canonical molecular orbitals of 1,2-$S_2N_3^+$ (**B**).

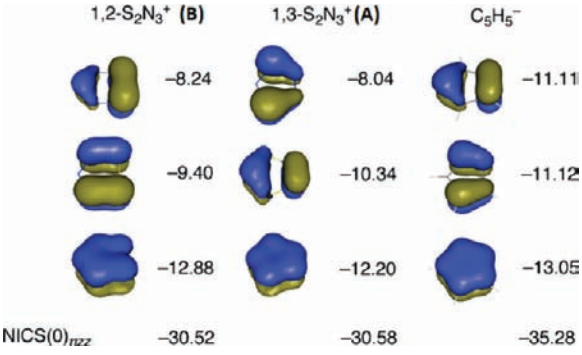


**Figure 10.** $NICS(0)_{zz}$ contributions (in ppm) of the schematically related $\pi$ canonical molecular orbitals (CMOs) of 1,2-$S_2N_3^+$ (**B**), 1,3-$S_2N_3^+$ (**A**) and $C_5H_5^-$. The $NICS(0)_{\pi zz}$ values are the sum of the three $\pi$ CMO-$NICS(0)_{zz}$ values.

**Table 3.** NICS Values (ppm) for 1,3-$S_2N_3^+$ (**A**), 1,2-$S_2N_3^+$ (**B**), $N_5^-$ (**C**), $SN_4$ (**D**), 1,3-$S_3N_2^{2+}$ (**E**), 1,2-$S_3N_2^{2+}$ (**F**), $C_5H_5^-$, and $C_6H_6$[a]

| | 1,3-$S_2N_3^+$ (**A**) | 1,2-$S_2N_3^+$ (**B**) | $N_5^-$ (**C**) | $SN_4$ (**D**) | 1,3-$S_3N_2^{2+}$ (**E**) | 1,2-$S_3N_2^{2+}$ (**F**) | $C_5H_5^-$ | $C_6H_6$ |
|---|---|---|---|---|---|---|---|---|
| NICS (0) | −18.9 | −23.3 | −16.5 | −19.5 | −21.6 | −20.7 | −12.9 | −7.5 |
| NICS (1) | −16.8 | −18.5 | −16.0 | −17.2 | −16.8 | −17.5 | −9.8 | −9.6 |
| $NICS(0)_\pi$ | −16.6 | −20.2 | −28.6 | −27.2 | −24.4 | −24.6 | −25.8 | −25.1 |
| $NICS(0)_{zz}$ | −45.4 | −54.0 | −43.5 | −47.6 | −48.9 | −45.2 | −17.3 | −15.0 |
| $NICS(0)_{\sigma zz}$ | −14.8 | −23.5 | −7.9 | −14.6 | −21.0 | −17.0 | +18.0 | +21.2 |
| $NICS(0)_{\pi zz}$ | −30.6 | −30.3 | −36.3 | −33.0 | −27.9 | −28.2 | −35.3 | −36.2 |

[a] Computed at the GIAO-MP2/6-311 + G(3df)//PW91/IGLOIII level. All of these species have six $\pi$ electrons (three occupied $\pi$ MOs). The isotropic NICS values were computed with NICS points located at the ring center, NICS(0), and 1 Å above, NICS(1). $NICS_\pi$ includes only contributions from the $\pi$ canonical molecular orbitals (CMOs). $NICS_{zz}$ are the extracted out-of-plane ($zz$) tensor components of the isotropic NICS, and be dissected into the respective sigma ($NICS_{\sigma zz}$) and $\pi$ ($NICS_{\pi zz}$) orbital contributions.

The dissected $NICS_\pi$[35−37] and $NICS_{\pi zz}$[32−34] indexes eliminate the sigma contamination effectively and only include the $\pi$ MO contributions. In agreement with $NICS_{\pi zz}$ (see above), the $NICS(0)_\pi$ values of (**A**) (−16.6) and (**B**) (−20.2) are slightly less negative than $C_5H_5^-$ (−25.8) and benzene (−25.1) (see also Table 3).

Both (**A**) and (**B**) are less aromatic than $C_5H_5^-$ and benzene because of their alternating S and N ring atoms. Figure 10 presents the schematically related $\pi$ CMOs of 1,3-$S_2N_3^+$ (**A**), 1,2-$S_2N_3^+$ (**B**) and $C_5H_5^-$ and their individual contributions to the overall $NICS(0)_{\pi zz}$ value. The HOMOs of (**A**) and **(B)** have less evenly distributed electron density and thus have slightly less negative $NICS(0)_{zz}$ values (−8.2 and −8.0 ppm, respectively) compared to the HOMO of $C_5H_5^-$ (−11.1 ppm). The $NICS(0)_{zz}$ values of the lower $\pi$ MOs of (**A**) and (**B**) are also less diatropic than those of $C_5H_5^-$. Hence, the resulting $NICS(0)_{\pi zz}$ values of (**A**) and (**B**) are less negative than $C_5H_5^-$.

The magnetic aromaticity of the other $S_xN_y$ species, $N_5^-$ (**C**), $SN_4$ (**D**), 1,3-$S_3N_2^{2+}$ (**E**), and 1,2-$S_3N_2^{2+}$ (**F**) valence isoelectronic with $C_5H_5^-$, also vary depending on the degree of ring atom alternation. The $NICS(0)_{\pi zz}$ values of (**C**)−(**F**) range from −28 ppm to −36 ppm. Note that species with more alternating ring atoms, (e.g., (**E**) (−27.9 ppm) and (**F**) ($NICS(0)_{\pi zz}$ = −28.2 ppm), are less negative (less aromatic), while those with less alternation have more negative $NICS(0)_{\pi zz}$ values (more aromatic). Thus, the $NICS(0)_{\pi zz}$ value of $N_5^-$ (**C**) (−36.3 ppm) is comparable to $C_5H_5^-$ (−35.3 ppm) and to benzene (−36.2 ppm) (see Table 3).

## 4. Conclusions

Despite being thermodynamically more stable than its known 1,2-$S_2N_3^+$ (**B**) isomer, 1,3-$S_2N_3^+$ (**A**) has not been observed. This is not an oversight of preparative chemistry but more likely is due to the facile dissociation of (**A**). The fragmentation of 1,3-$S_2N_3^+$ (**A**) into $SNS^+$ and $N_2$ is computed to have a very low dissociation barrier (2.6 kcal/mol at the MP2/6-311 + G(3df) level). In contrast, all of the possible dissociation pathways of the metastable (but viable) 1,2-$S_2N_3^+$ (**B**) have higher dissociation barriers. Thus, 1,2-$S_2N_3^+$ (**B**) is more "stable" (kinetically more persistent) than 1,3-$S_2N_3^+$ (**A**), but (**A**) is more "stable" (thermodynamically, having lower energy) than (**B**). This emphasizes the need to use the word "stable" with circumspection in scientific contexts.[46] On the basis of $NICS(0)_{\pi zz}$ computations, both 1,2- and 1,3-$S_2N_3^+$ are almost as aromatic as the valence isoelectronic $C_5H_5^-$, despite their bond length alternation and nonuniformity of the ring S and N atoms. Likewise, the aromaticity of the six $\pi$ electron 1,2- and 1,3-$S_3N_2^{2+}$ rings also are weakened slightly, compared to $C_5H_5^-$. Note that aromaticity not only contributes to the thermochemical stability of ground states but also can lower the energy of pericyclic cycloreversion transition states.[27b] Although being as aromatic as $C_5H_5^-$, the pure nitrogen $N_5^-$ ring decomposes readily.

**Acknowledgment.** This paper is dedicated to Yitzhak Apeloig on the occasion of his 65th birthday. Support by the National Natural Science Foundation of China (Grant 10274015), the Science Foundation of Harbin Institute of Technology, China, and the National Science Foundation (U.S.A.) Grant 0716718 are gratefully acknowledged. Some computations were performed at the National Laboratory of Theoretical and Computational Chemistry, Jilin University, China.